Inorganica Chimica Acta 423 (2014) 194–203

Contents lists available at ScienceDirect

Inorganica Chimica Acta

journal homepage: www.elsevier.com/locate/ica

Characterization, antibacterial, anticarbonic anhydrase II isoenzyme, anticancer, electrochemical and computational studies of sulfonic acid hydrazide derivative and its Cu(II) complex

Ümmühan Ö. Özdemir [a,*], Ebru Aktan [a], Firdevs İlbiz [a], Ayla B. Gündüzalp [a], Neslihan Özbek [b], Musa Sarı [c], Ömer Çelik [d], Sinan Saydam [e]

[a] Department of Chemistry, Faculty of Science, Gazi University, Ankara, Turkey
[b] Department of Chemistry, Faculty of Education, Ahi Evran University, Kırşehir, Turkey
[c] Department of Physics Education, Gazi University, Ankara, Turkey
[d] Department of Physics Education, Dicle University, Diyarbakır, Turkey
[e] Department of Chemistry, Faculty of Science, Fırat University, Elazığ, Turkey

ARTICLE INFO

Article history:
Received 15 July 2014
Received in revised form 18 September 2014
Accepted 23 September 2014
Available online 7 October 2014

Keywords:
Butane sulfonic acid hydrazide
Cu(II) complex
Biological activities
Electrochemical studies
Crystal structure
DFT

ABSTRACT

A new N′-acetyl butane sulfonic acid hydrazide, C_4H_9-SO_2-NH-NH-$COCH_3$ (Absh, an sulfonamide compound), and its Cu(II) complex $[Cu(Absh)_2(CH_3COO)_2]$, have been synthesized and characterized by elemental analysis, spectrometric methods (^1H–^{13}C NMR, FT-IR, LC–MS), thermal analysis, magnetic susceptibility and conductivity measurements. In addition, molecular structure of the ligand, Absh was determined by single crystal X-ray diffraction technique and found that the compound crystallizes in monoclinic, space group $P2_1/c$. To gain information about the structure of the ligand and its complex, we have performed computational studies using density functional theory (DFT) for optimized geometries of the compounds. Electrochemical studies showed that, the complex is electrochemically active and has one irreversible reduction and one irreversible oxidation potentials, and the half wave reduction potentials are −1.15 and 0.45 volt respectively, versus ferrocene/ferrocenium internal reference electrode. The antibacterial activities of synthesized compounds were studied against Gram positive bacteria; *Staphylococcus aureus* ATCC 6538, *Bacillus subtilis* ATCC 6633, *Bacillus cereus* NRRL-B-3711, *Enterococcus faecalis* ATCC 29212 and Gram negative bacteria; *Escherichia coli* ATCC 11230, *Pseudomonas aeruginosa* ATCC 15442, *Klebsiella pneumonia* ATCC 70063 by using the disc diffusion and micro dilution methods. The inhibition activities of these compounds on carbonic anhydrase II enzyme (hCA II) have been investigated by comparing IC_{50} and K_i values. The anticancer activities of these compounds on MCF-7 cell line investigated by comparing IC_{50} values. The biological activity screening showed that Cu(II) complex has more activity than ligand against the tested bacteria, hCA II enzyme and breast cancer cell lines MCF-7.

1. Introduction

Sulfonamides and their derivatives are extensively used in human and veterinary medicine [1]. It has been extensively used as antimicrobial [2], antifungal [3], antimalarial [4], antitumor activity [5,6] and carbonic anhydrase inhibitors (as diuretic or hypoglycaemic reagents) [7–9] and, still there is considerable interest. It also as used as pharmaceutical agents for the treatment of different diseases such as infections [10] Alzheimer's disease [11] and HIV [12]. The molecules of sulfonic acid hydrazide involve two pharmacophoric fragments: sulfonamide group and hydrazine residue. Some of them exhibit strong cytostatic activity [13,14], antibacterial [15] anti-inflammatory and analgesic [16,17] activity, as well as carbonic anhydrase activating properties [18]. To find better compounds, some metal sulfonamides have attracted much attention due to the fact that complexes showed more activity than free ligands. In particular, Ag-sulfadiazine has proved to be an effective topical antimicrobial agent of significance in burn therapy, and better than the free ligand or $AgNO_3$ [19]. Moreover, it has been found that, several Cu(II), Ce(III), Bi(III), Cd(II), and Hg(II) sulfonamide complexes have revealed antibacterial activity [20,21]. Transition metal complexes of hydrazides and sulfonamides as well as their hydrazone derivatives also find application in chemotherapy [22]. Due to significant applications of sulfonamides/sulfonylhydrazines/sulfonylhydrazones in pharmacology

* Corresponding author. Fax: +90 312 2122279.
E-mail address: ummuhan@gazi.edu.tr (Ü.Ö. Özdemir).

http://dx.doi.org/10.1016/j.ica.2014.09.033
0020-1693/

and widespread use in medicine, these compounds have gained importance in bio-inorganic and metal based drug chemistry.

In our previous studies, we reported the antibacterial and cytotoxic effect of methane sulfonic acid hydrazide ($CH_3SO_2NHNH_2$) and its sulfonyl hydrazone derivatives [23,24], as well as its metal complexes [25,26]. Methane, ethane and propanesulfonylhydrazone derivatives and their transition metal complexes were synthesized and screened for their antimicrobial activities [27–29]. Furthermore, ethanesulfonylhydrazone derivatives and their transition metal complexes, and different aromatic/hetero aromatic sulfonylhydrazone derivatives were investigated for inhibitory effects on carbonic anhydrase II (hCA II) enzyme [28,30].

As part of our ongoing studies, N′-acetyl butane sulfonic acid hydrazide (Absh) and its Cu(II) complex were synthesized for the first time and characterized by using elemental analysis, $^1H/^{13}C$ NMR, FT-IR, LC–MS, UV–Vis spectrometric methods, magnetic susceptibility, conductivity measurements, thermal studies and X-ray crystallography method for compounds. The antibacterial activities of synthesized compounds were studied against Gram positive bacteria; *Staphylococcus aureus* ATCC 6538, *Bacillus subtilis* ATCC 6633, *Bacillus cereus* NRRL-B-3711, *Enterococcus faecalis* ATCC 29212 and Gram negative bacteria; *Escherichia coli* ATCC 11230, *Pseudomonas aeruginosa* ATCC 15442, *Klebsiella pneumonia* ATCC 70063 by using the disc diffusion and micro dilution methods. The inhibition activities of these compounds on carbonic anhydrase II enzyme (hCA II) have also been investigated by comparing IC_{50} and K_i values. In addition anticancer activities of these compounds on MCF-7 cell line investigated by comparing IC_{50} values. The electrochemical behaviors of ligand and its Cu(II) complex were evaluated by cyclic voltammetry (CV). The structure of the ligand was optimized using 6–311G(d,p) functional in which B3LYP functional were implemented. The geometry of the complex was optimized at the DFT level by using the UB3LYP method and LANL2DZ basis set. These global reactivity descriptors such as ionisation potential ($I = E_{HOMO}$), electron affinity ($A = E_{LUMO}$), energy band gap ($\Delta E = E_{HOMO} - E_{LUMO}$), electronegativity ($\chi = I + A/2$), chemical potential ($\mu = -\chi$), global hardness ($\eta = I - A/2$), global softness ($S = 1/\eta$) and global electrophilicity index ($\omega = \mu^2/2\eta$) were determined with GAUSSIAN 09 program.

2. Experimental

2.1. Physical measurements

The crystal structure of N′-acetyl butane sulfonic acid hydrazide (Absh) was determined by using a on a Bruker Kappa APEX II CCD area-detector. The solvents used were purified and distilled according to routine procedures. Butane sulfonyl chloride, hydrazine hydrate, and cupper acetate were commercial products (purum). Elemental analyses were performed according to standard micro analytical procedures by Leco CHNS-932, ^1H and ^{13}C NMR spectra of dimethylsulfoxide-d_6 (DMSO-d_6) solutions of the compounds were registered on a Bruker WM-400 spectrometer (400 MHz) using tetra methyl silane as internal standard. The infrared spectra of the compounds as KBr-disks were recorded in the range of 4000–400 cm^{-1} with a Mattson 1000 FT spectrometer. UV–Vis spectra were recorded on UNİCAM-UV 2–100 spectrophotometer. Melting points of sulfonamide derivatives were determined with a Gallenkamp melting point apparatus. The molar magnetic susceptibilities were measured on powdered samples using Gouy method. The molar conductance measurements were carried out using a Siemens WPA CM 35 conductometer. Cyclic voltammograms (CV) were carried out using a Gamry Reference 600 Potentiostat/Galvanostat/ZRA. The microdilution broth and disc diffusion method were used to determine the antibacterial activity of compounds against Gram positive bacteria; *S. aureus* ATCC 6538, *B. subtilis* ATCC 6633, *B. cereus* NRRL-B-3711, *E. faecalis* ATCC 29212 and Gram negative bacteria; *E. coli* ATCC 11230, *P. aeruginosa* ATCC 15442, *K. pneumonia* ATCC 70063. The inhibition activities of synthesized compounds on carbonic anhydrase II (hCA II) have been investigated by comparing K_i and IC_{50} values.

2.2. Synthesis of ligand (Absh) and its Cu(II) complex

The nucleophilic substitution reaction of the of hydrazine hydrate with butane sulfonyl chloride was carried out as follows: An ethanol solution of butane sulfonyl chlorides (C_4H_9-SO_2Cl) was added dropwise to the ethanol solution of hydrazine hydrate (0.12: 0.62 equiv), maintaining the temperature between 10 and 12 °C. Then, the reaction mixture was stirred for 1 h at room temperature. After the completion of the reaction, the solvent was removed under vacuum and the viscose residue was taken to ether phase using a continuous extraction method. Then the ether was removed with rotary evaporator. The resulting product was boiled with ethyl acetate and then allowed to stand in the freezer. Bright transparent crystals were obtained after a few weeks. Calc. for $C_6H_{14}N_2O_3S$: C, 37.09; H, 7.26; N, 14.42; O, 24.71; S, 16.51. Found: C, 35.87; H, 7.18; N, 13.98; O, 23.53; S, 16.00%. Yield: 70%, M.p. 45–48 °C.

The synthesis of the cupper complex was performed as follows; 30 ml of acetonitrile was added to a 100 ml of two neck flask equipped with a condenser. Solvent was purged with argon for five minutes then 0.250 g (1.27 mmol) of ligand transferred to the flask at room temperature, followed by the addition of 0.253 gram of copper(II)acetate monohydride (1.27 mmol). The solution was left to reflux for 24 h, after then the blue solution was filtered and left for crystallization. After 5 days at room temperature, blue crystals were formed (0.310 g). The complex is soluble in acetonitrile, THF, DMF. Calc. for $C_{16}H_{34}N_4O_{10}S_2$ Cu; C, 33.71; H, 6.01; N, 9.83; O, 28.06; S, 11.25. Found: C, 32.87; H, 5.70;N, 8.98; O, 25.66; S, 11.20%. Yield: 70%, M.p. 230 °C.

2.3. X-ray structure determination

Crystallographic data of the ligand Absh were recorded on a Bruker Kappa APEX II CCD area-detector X-ray diffractometer using graphite monochromatized with Mo Kα radiation ($\lambda = 0.71073$ Å), using $\omega - 2\theta$ scan mode. The empirical absorption corrections were applied by multi-scan via Bruker, SADABS software [31]. The structures were solved by the direct methods and refined by full-matrix least-squares techniques on F^2 using the solution program SHELXS-97 and refined using SHELXL-97 [32]. All non-hydrogen atoms were refined with anisotropic displacement parameters. Hydrogen atoms bonded to the carbon and nitrogen atoms were placed in calculated their idealized positions and refined as riding, with C–H = 0.96–0.97 Å and N–H = 0.82–0.86 Å with $U_{iso}(H) = 1.2\ U_{eq}(C,N)$. The molecular structure plots were prepared using ORTEP-3 for Windows [33]. The crystal and instrumental parameters used in the unit-cell determination and data collection are summarized in Table 1 for the compounds.

2.4. Theoretical calculations

The structure of the ligand Absh was optimized using 6–311G(d,p) functional in which B3LYP functional were implemented [34,35]. The geometry of the complex was optimized at the DFT level by using the UB3LYP method and LANL2DZ basis set [36]. The vertical electronic excitations of the complex based on B3LYP optimized geometries were computed using the time-dependent density functional theory (TD-DFT), formalism in acetonitrile using the integral equation formalism polarizable continuum model

Table 1
Crystal data and structure refinement details for Absh molecule.

	1
Empirical formula	$C_6H_{14}N_2O_3S$
Formula weight	194.26
T (K)	296(2)
λ (Å)	0.71073
Crystal system	monoclinic
Space group	$P2_1/c$
Unit cell dimensions	
a (Å)	6.736(3)
b (Å)	15.965(6)
c (Å)	9.513(4)
β (°)	102.47(2)
V (Å^3)	998.9(7)
Z	4
Absorbtion coefficient (mm^{-1})	0.299
D_{calc} (Mg m^{-3})	1.292
$F(000)$	416
Crystal size (mm)	0.22 × 0.15 × 0.12
θ range for data collection (°)	2.80–31.72
Index ranges	$-9 \leqslant h \leqslant 9$, $-15 \leqslant k \leqslant 23$, $-3 \leqslant l \leqslant 14$
Reflections collected	15267
Independent reflections	3384
Data/parameters	2734/119
Maximum and minimum transmission	0.948, 0.965
Final R indices [$I \geqslant 2(I)$]	$R_1 = 0.0583$, $wR^2 = 0.1446$
R indices (all data)	$R_1 = 0.0734$, $wR^2 = 0.1605$
Goodness-of-fit (GOF) on F^2	1.104
Largest difference in peak and hole (e Å^{-3})	0.247and −0.665

(IEFPCM) [37] using the B3LYP level and LANL2DZ basis sets. Molecular orbitals energies (HOMO–LUMO) of ligand and its Cu(II) complex have been calculated. The vibrational frequency calculations show that the optimized structures are on real local minima without imaginary frequencies. All the DFT calculations were performed with the GAUSSIAN G09 program package [38]. The $^1H/^{13}C$ NMR chemical shifts of the Absh (L) were computed at the DFT/B3LYP/6–311++G(2d,2p) level of theory in DMSO by applying the (GIAO) approach [39] and the values for the $^1H/^{13}C$-isotropic were referenced to TMS, which was calculated at the same level of theory.

2.5. Biological activity

2.5.1. Procedure for antibacterial activity

The in vitro antibacterial activity of the free the ligand, Absh, and its complex were tested against the Gram positive bacteria; *S. aureus* ATCC 25923, *B. subtilis* RSKK 244, *Bacillus megaterium* RSKK 5117 and Gram negative bacteria, *Salmonella enteritidis* ATCC 13076, *E. coli* ATCC 11230. The *Bacteria* cultures were obtained from Gazi University, Biology Department. Bacterial strains were cultured overnight at 310 K in Nutrient Broth. During the survey, these stock cultures were stored in the dark at 277 K. The inocula of microorganisms were prepared from 12 h broth cultures and suspensions were adjusted to 0.5 McFarland standard turbidity.

2.5.1.1. Disc diffusion method. The ligand and complex were dissolved in dimethylsulfoxide (20% DMSO) to a final concentration of 5.0 mg mL^{-1} and sterilized by filtration by 0.45 μm Millipore filters. Antimicrobial tests were then carried out by the disc diffusion method using 100 μL of suspension containing 10^8 CFU mL^{-1} bacteria spread on a nutrient agar (NA) medium. The discs (6 mm in diameter) were impregnated with 20 μL of each compound (100 μg/disc) at the concentration of 5.0 mg mL^{-1} and placed on the inoculated agar. DMSO impregnated discs were used as negative control. Sulfamethoxazole (300 μg/disk) and sulfisoxazole (300 μg/disk) were used as positive reference standards to determine the sensitivity of one strain/isolate in each microbial species tested. The inoculated plates were incubated at 37 °C for 24 h for bacterial strains isolates. Antimicrobial activity in the disc diffusion assay was evaluated by measuring the zone of inhibition against the test organisms. Each assay in this experiment was repeated twice. Percentage of inhibition by comparing distance of the compounds to the positive control using (sulfamethoxazole) the equation below [40].

$$\%\ \text{Inhibition} = \left[\frac{\text{diameter of the sample}}{\text{diameter of the positive control}}\right] \times 100$$

2.5.1.2. Micro dilution assays. The inocula of microorganisms were prepared from 12 h broth cultures and suspensions were adjusted to 0.5 McFarland standard turbidity. The test compounds dissolved in 20% dimethylsulfoxide (DMSO) were first diluted to the highest concentration (8.0 mg mL^{-1}) to be tested, and then serial, twofold dilutions were made in a concentration range from 15.625 to 4000 μg mL^{-1} in 10 ml sterile test tubes containing nutrient broth. The MIC values of each compound against bacterial strains were determined based on a micro-well dilution method. The 96-well plates were prepared by dispensing 95 μL of nutrient broth and 5 μL of the inoculums into each well. One hundred microliter from each of the test compounds initially prepared at the concentration of 4000 μg mL^{-1} was added into the first well. Then, 100 μL from each of their serial dilutions was transferred into nine consecutive wells. The last well containing 195 μL of nutrient broth without compound, and 5 μL of the inoculum on each strip, was used as negative control. The final volume in each well was 200 μL. The contents of the wells were mixed and the micro plates were incubated at 37 °C for 24 h. All compounds tested in this study were screened twice against each microorganism. The MIC was defined as the lowest concentration of the compounds to inhibit the growth of microorganisms [41]. The results were compared with a similar run of sulfamethoxazole and sulfisoxazole as an antibacterial.

2.5.2. Procedure for CA II enzyme inhibitor activity

Carbonic anhydrase activity was assayed by the hydrolysis of p-nitrophenylacetate [42]. IC_{50} and K_i values of compounds were determined on hCA II enzyme. Acetazolamide (5-acetamido-1,3,4-thiadiazole-2-sulfonamide) AAZ, a clinically used in hCA II inhibition has also been investigated as standard inhibitor.

In order to determine IC_{50} values, 100 μL of 3.0 mM p-nitrophenylacetate as substrate and four different concentrations (3×10^{-2}; 3×10^{-3}; 5×10^{-4}; 3×10^{-4} M) of inhibitors (Ligand and Cu(II) complex) were used. Reaction was started by adding of 170 μL of 0.05 M tris–SO_4 buffer (pH 7.6) and 0.1 μL enzyme solution for total volume of 300 μL. The absorbance was determined at 348 nm after 6 min [43]. This study was repeated three times for each inhibitor. In order to determine IC_{50} values, Graphs were drawn by using % inhibition values by a statistical packing program on a computer. The IC_{50} concentrations of the compounds were determined from graphs [44]. This method was applied to determine K_i values. In the media with or without inhibitor, the substrate concentrations were 0.3, 0.6, 1.0, 3.0 mM. For this aim, inhibitor solutions were used for the reaction medium in four different concentrations (3×10^{-2}; 3×10^{-3}; 5×10^{-4}; 3×10^{-4} M). The Lineweaver-Burk graphs were obtained and K_i values were calculated according to *Cheng Prusoff* equation.

2.5.3. Cell culture and cytotoxicity determination

The cells were incubated under 5% CO_2/air at 37 °C conditions at Nuaire humidified carbon dioxide incubator (Plymouth, MN, USA).

Cells' state was controlled by inverted microscope (Soif Optical Inc., China) and results are expressed as mean ± STD. Statistical analysis and comparison between mean values for cytotoxicity were performed by Tukey variance analysis (SPSS 10.0 for Windows; Chicago, IL, USA).

2.5.3.1. MTT assay. A colorimetric cell viability assay under usage of the tetrazole 3-(4,5-dimethylthiazol-2yl)-2,5-diphenyltetrazolium bromide (MTT) was used to evaluate the cytotoxic effects of the test compounds [45]. MCF-7 cancer cell line were grown as monolayer culture in a high glucose concentration (4.5 g/l) DMEM medium supplemented with 10% fetal calf serum (FCS), 1% L-glutamine (200 mM), 1% of mixture penicillin (100 IU/ml) and streptomycin (100 lg/ml) incubated at 37 °C in an atmosphere of 5% CO_2–95% air mixture. Briefly, $5x10^4$ MCF-7 tumor cells were plated in triplicate in 96-well flat bottom tissue culture plates, and treated with different concentrations of drugs for the time indicated. MTT (0.005 g = ml in phosphate buffer saline) was added to the cell culture and incubated for 4 h at 37 °C in 5% CO_2 humidified incubator. The formazan crystals formed during the reaction of active mitochondria with MTT, were dissolved in 0.04 N (100 ml) in isopropanol and readings were taken in a microtiter plate reader using a 570 nm filter. The results were compared with a similar run of docetaxel as an antitumor compound.

2.6. Electrochemistry experimental

All chemicals used were reagent grade. The solvents were purified according to standard procedure [46] and stored over molecular sieves. Electrochemical grade tetra butyl ammonium tetra fluoro borate (TBAFB) (Fluka) was used as the supporting electrolyte in voltammetric measurements in non–aqueous solvents. Cyclic voltammograms (CV) were carried out using a Gamry Reference 600 Potentiostat/Galvanostat/ZRA. A three electrode system was used for CV measurements in dimethylformamide (DMF) consist of glassy carbon working electrode, and a platinum wire counter and platinum wire quasi–reference electrode. The ferrocene/ferrocenium couple (Fc/Fc^+) was used as an internal standard and potentials reported with respect to Fc/Fc^+ in non-aqueous solutions. High purity Argon is used for the de-oxygenation of the cell at least 10 min prior to electrochemical measurements and the solution was protected from air by a blanket of argon during the experiments.

3. Results and discussion

The elemental analysis results show 1:2 (metal:ligand) stoichiometry for the complex. The analytical results are in good agreement with those required by the general formula [$(ML_2(CH_3COO)_2$]. The molar conductivity (Λ_m) of 10^{-3} M solutions of the complex in DMSO at 25 C were measured and the Cu(II) complex were found non-electrolytic (12.5 Ω^{-1} cm^2 mol^{-1}) [47,48].

3.1. Crystal structure of Absh

Crystals of Absh were obtained by the slow evaporation of its ethyl acetate solution. Molecular structure and crystal data's of the title compound presented in Fig 1 and Table 1. Compound Absh crystallized in the $P2_1/c$ space group. The S–O and S–N bond distances lie within expected range of 1.4313(17)–1.4344(17) Å and 1.6514(18) Å, respectively. All bond lengths and angles for compound are consistent with those found in related compounds [49,27] (Table 2) .

3.2. The characterization of compounds

3.2.1. IR spectra

Bands in the region of 3197 and 3243 cm^{-1} [50] may be due to ν(NH) stretching vibration for Absh. Upon complexation, the ν(NH) stretching vibration shifts to lower frequency, suggesting coordination through nitrogen atom. The strong band at 1669 cm^{-1} is assigned to ν(C=O) stretching mode for ligand. This band shifts to lower wave number in Cu(II) complex. These shifts support the participation of the NH and C=O group of this ligand in binding to the metal ion [51,52].

Several new bands present in the region of 1610 and 1415 cm^{-1} which are assigned to $\nu_{as}(COO^-)$ and $\nu_s(COO^-)$ stretching vibrations of the acetato ligand, respectively. The wave number separation value between these two bands, $\Delta\nu = 205$ cm^{-1}, is characteristic of a monodentate acetato ligand in this complex [53–55]. And also, new bands present in the region 400–600 cm^{-1} were assigned to Cu–N and Cu–O stretching vibrations [56]. Ligand also displays bands at 1342 and 1160 cm^{-1} which are assigned to $\nu_{as}(SO_2)$ and $\nu_s(SO_2)$ stretching vibrations, respectively. In the spectrum of complex, the position of these bands remained largely unchanged, suggesting that the SO_2 group of ligand is not involved in coordination to the metal [57].

3.2.2. NMR spectra

^1H–^{13}C NMR spectra of compound Absh were obtained in DMSO-d_6 at room temperature using TMS as an internal standard. ^1H–^{13}C NMR Chemical shifts of the ligand molecule Absh were calculated by Gauge-Independent Atomic Orbital (GIAO) method [39] at DFT/B3LYP/6–311++G(2d,2p) level in DMSO. The experimental and calculated ^1H–^{13} NMR assignments in DMSO-d_6 are listed in Table 3. The correlation coefficient (R^2) of experimental and calculated ^1H and ^{13}C chemical shift values were obtained as the same (0.988).

The CH_3 protons of butyl moiety, (H1) and the CH_3 protons of acetyl moiety, (H6) are easily distinguishable as a singlet, and they are observed at 0.85 and 1.82 ppm, and corresponding calculation values are 1.09 and 2.07 ppm, respectively. The CH_2 protons of butyl moiety, H2, H3, H4 (two H intensities) are observed at 1.34, 2.49 and 2.98 ppm, and corresponding calculation values are 1.35, 2.00 and 3.26 ppm, respectively. In addition, the H13 and H14 on the nitrogen atoms (one H intensities) are observed at 9.27 and 9.97 ppm which are attributed to the NH (binding to acetyl group) and NH (binding to metal atom) protons, and corresponding calculation values are 7.13 and 7.71 ppm respectively.

The CH_3 carbon of butyl moiety, (C1) and the CH_3 carbon of acetyl moiety, (C6) are observed at 13.92 and 21.38 ppm, and corresponding calculation values are 16.09 ppm and 22.15 ppm, respectively. The CH_2 carbons of butyl moiety, C2, C3, C4 are observed at 25.38, 39.89, 51.59 ppm and corresponding calculation values are 27.13, 30.84 and 63.05 ppm, respectively. The carbon peak (C5) in Absh is found at 169.34 ppm and corresponding calculated value is 177.44 ppm.

3.2.3. Mass spectrometry

The electron impact mass spectrum of the Cu(II) complex was recorded at 70 eV. Cu(II) complex has molecular ion peak, $[M]^+$ at 569 (10%), m/z (intensity %) corresponding to $[Cu(Absh)_2(CH_3COO)_2]^+$ fragmentation routes as shown in Fig. 2.

The first fragment is traced by a peak at m/z 337(20%) owing to elimination of two acetate, $2(CH_3COO)$, and two butyl, $2(C_4H_9)$ moieties from the complex. Then, the other fragments with the separation of the two SO_2 (one by one) and a CH_3 groups are observed at m/z 272 (27%), 208(16%) and 191(38%), respectively. Finally, the fragments by removing of the CO group and after also $COCH_3$ group occur at m/z 167(100%) and 125 (100%) as the main peaks.

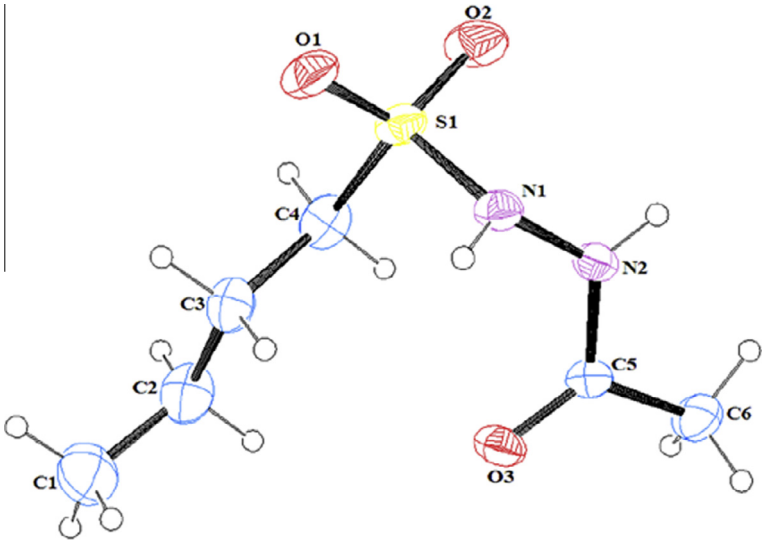

Fig. 1. The molecular structure of Absh showing the atom-labelling scheme.

Table 2
Experimental and calculated structural parameters (bond length in Å, angles in °) of Absh molecule.

Bond length			Bond angle			Torsion angle		
	Exp.	Calc.		Exp.	Calc.		Exp.	Calc.
C1–C2	1.505(5)	1.531	C1 C2 C3	112.8(3)	112.4	C1–C2–C3–C4	−176.9(3)	−179.9
C2–C3	1.525(4)	1.535	C2 C3 C4	113.0(2)	111.6	C2–C3–C4–S1	−171.00(19)	176.5
C3–C4	1.522(4)	1.525	O1 S1 C4	108.91(12)	109.1	C3–C4–S1–O1	−41.7(2)	−42.8
S1–C4	1.780(3)	1.820	O1 S1 O2	119.67(11)	122.6	C4–S1–N1–N2	66.76(15)	62.4
S1–O1	1.430(18)	1.456	O1 S1 N1	104.43(9)	103.7	O1–S1–N1–N2	−177.23(13)	178.1
S1–O2	1.435(18)	1.457	O2 S1 N1	105.76(11)	105.0	O2–S1–N1–N2	−50.09(15)	−52.1
S1–N1	1.650(19)	1.731	N2 N1 S1	115.73(12)	115.3	S1–N1–N2–C5	−99.20(18)	−106.3
N1–N2	1.391(2)	1.392	C5 N2 N1	121.25(15)	120.9	O2–S1–C4–C3	−173.95(18)	−177.7
N2–C5	1.353(2)	1.375	O3 C5 N2	122.03(18)	121.4	N1–S1–C4–C3	71.3(2)	69.4
C5–O3	1.231(2)	1.219	O3 C5 C6	123.23(17)	123.5	N1–N2–C5–O3	1.4(3)	−171.3
C5–C6	1.494(3)	1.512	N2 C5 C6	114.72(17)	115.0	N1–N2–C5–C6	−176.99(18)	−171.3

Table 3
Comparison of calculated and experimental values of ^{1}H and ^{13}C NMR chemical shifts (ppm) relative to TMS in DMSO for the Absh molecule.

^{1}H NMR			^{13}C NMR		
Atom no.	Exp.	Calc.	Atom no.	Exp.	Calc.
H14	9.97	7.71	C6	21.38	22.15
H13	9.27	7.13	C5	169.34	177.44
H6	1.82	2.07	C4	51.59	63.05
H4	2.98	3.26	C3	39.89	30.84
H3	2.49	2.00	C2	25.38	27.13
H2	1.34	1.35	C1	13.92	16.09
H1	0.85	1.09			

3.2.4. Electronic spectra and magnetic behavior

The electronic absorption spectra are often very helpful in the evaluation of results furnished by other methods of structural investigation. The here for, the electronic spectral measurements are used for assigning the stereochemistries of metal ions in the complex based on the positions and the number of *d–d* transition peaks. The electronic absorption spectrum of Cu(II) complex was recorded at room temperature using acetonitrile as solvent. Only one broad band is observed at 670 nm (14,925 cm^{-1}) in the electronic spectrum of the Cu(II) complex assigned to $^{2}E_g \rightarrow {}^{2}T_{2g}$ transition which is in conformity with distorted octahedral geometry [58].

The theoretical and experimental absorption wavelengths are obtained in acetonitrile having dielectric constants, $\varepsilon = 35.688$ Debye. The maximum absorption value of the complex is obtained experimentally at 670 nm and corresponding calculated value is 677 nm.

The magnetic moment of the octahedral complex (as B.M.) was measured at room temperature. The effective magnetic moment values for Cu(II) complex is 1.98 B.M. which is characteristic for this type of Cu(II) complex [59,60].

3.2.5. Thermal studies

The Cu(II) complex was left in glass oven at 170 °C for a 2 h in vacuo to prevent the hydration. The thermograms of anhydrous complex was observed in the range of 35–700 °C. As expected, there was no mass loss up to 230 °C. Cu(II) complex has thermally decompose in the range of 230–700 °C which means this complexes does not contain any coordinated or crystal water molecules.

3.3. Theoretical calculations

The experimental and optimized geometric parameters using DFT/B3LYP method with 6–311G(d,p) basis set for ligand are presented in Table 2. The geometric parameters are fairly consistent with the X-ray crystal structure results (Fig 1). We have obtained $R^2 = 0.988$ for the bond lengths and $R^2 = 0.978$ for the bond angles. The largest deviation was found for S1–N1 bond length as 0.081 Å and for O1–S1–O2 bond angle as 2.89°.

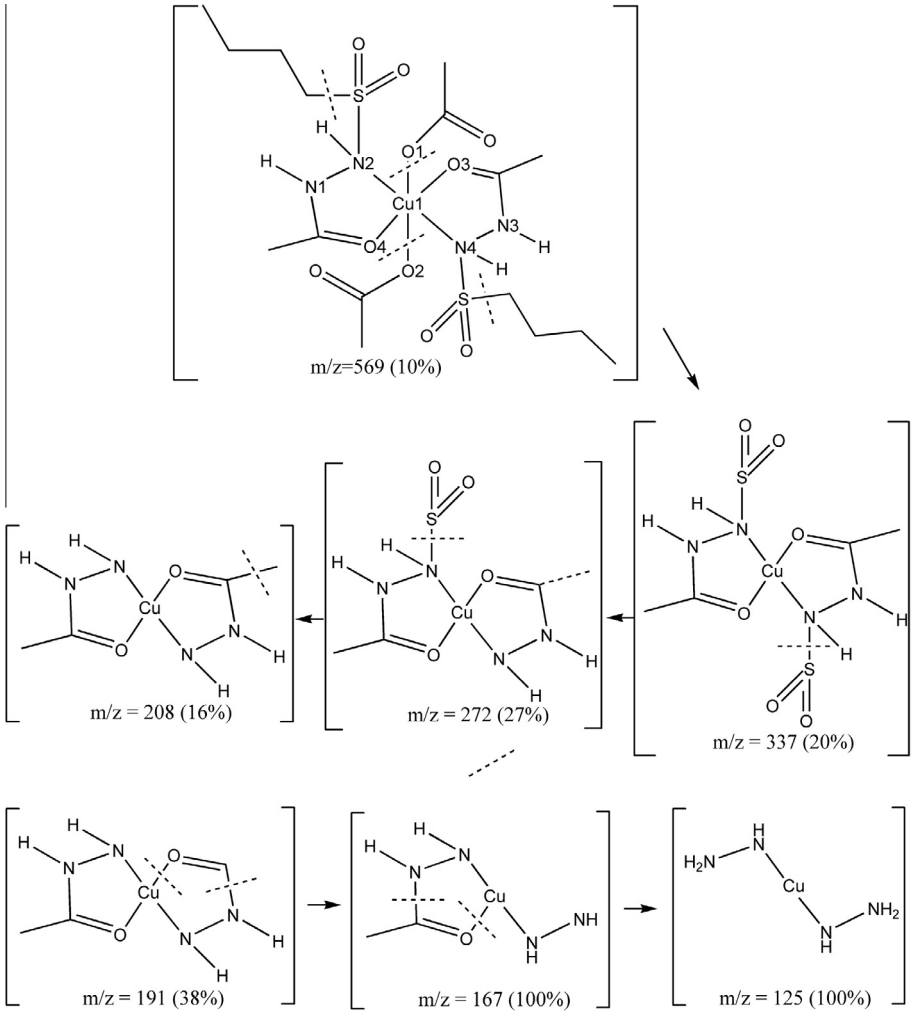

Fig. 2. Fragmentation pattern of $Cu[L_2(CH_3COO)_2]$ complex.

Some important bond lengths and angles around the central ion of the Cu(II) complex are shown in Table 4. Cu(II) ion coordinates through nitrogen and oxygen atoms of two Absh ligands and oxygen atoms of two acetate ions. In distorted octahedral geometry, two acetate ions are coordinated to the Cu(II) ion in the same plane. *Trans* and *cis* isomeric forms of the complex were calculated in the terms of energy and *trans* isomer was found to be more stable (ΔE = 2.90 kcal/mol) than *cis* isomer.

The highest occupied molecular orbitals (HOMO/SOMO) and the lowest unoccupied molecular orbitals (LUMO) of the ligand and its Cu(II) complex were calculated by B3LYP method using 6–311G(d,p) and LANL2DZ basic sets, respectively. The energy gap values between the molecular orbitals of ligand and complex are 6.92 eV for the ligand and 4.95 eV for the Cu(II) complex. The orbital densities around the atoms indicate which groups are responsible for the antibacterial activities [52]. HOMO/SOMO and LUMO of both compounds are located on the whole molecule except butyl group.

3.3.1. MEP and reactivity descriptors

The reactive sites of the molecules can be seen on the molecular electrostatic potential (MEP) surfaces which indicates the probable sites readily available for the electrophilic and nucleophilic reactions. Red zones indicate the most negative potentials correspond to electron-rich regions while blue zone indicate the most positive potentials correspond to electron-rich regions. The highest density of electrons is located around oxygen atoms. Ionisation potential ($I = -E_{HOMO}$), electron affinity ($A = -E_{LUMO}$), energy band gap ($\Delta E = E_{HOMO} - E_{LUMO}$), electronegativity ($\chi = I + A/2$), chemical potential ($\mu = -\chi$), global hardness ($\eta = I - A/2$), global softness ($S = 1/\eta$) and global electrophilicity index ($\omega = \mu^2/2\eta$) are listed in Table 5. These global reactivity descriptors are useful in predicting global chemical reactivity trends.

The correlations between electronic descriptors and antimicrobial activities show that Cu(II) complex has the highest activity than ligand. The calculated values of electronic features of the complex are affected by the conformations and we used the most stable conformations with the lowest energy.

Table 4
Selected calculated structural parameters (bond length in Å, angles in °) of the Cu(II) complex.

Bond length		Bond angle	
Cu1–O3	2.104	O2–Cu1–N4	89.152
Cu1–O1	1.979	O2–Cu1–N2	88.819
Cu1–O4	2.089	O2–Cu1–O4	90.456
Cu1–O2	1.958	O2–Cu1–O3	89.136
Cu1–N2	2.407	O1–Cu1–O4	87.596
Cu1–N4	2.382	O1–Cu1–N4	88.858
Torsion angle		O1–Cu1–N2	93.317
N2–Cu1–N4–N3	37.868	O1–Cu1–O3	92.939
N4–Cu1–N2–N1	149.139		

The electronic descriptors (such as HOMO/SOMO, LUMO, ΔE, χ, μ, η, S, w) (see Table 5) were calculated to find the effect of the chemical properties on the antibacterial, anticancer, anticarbonic anhydrase II activities of the compounds. The orbital densities around the atoms indicate which groups are responsible for the biological activities. The frontier molecular orbitals have the highest density around the sulfonamide groups and also acetyl sites which responsible for the activity of the compounds. The biological activities increase by increasing of HOMO, χ, S, w descriptors and by decreasing of LUMO, ΔE, μ, η descriptors. These components of the frontier molecular orbitals play an important role in activities. LUMO energy is the most important descriptors which describes electrophilicity of the compound, and its level has the importance because of the donor–acceptor interactions. In general, molecules with low LUMO energy values accept the electrons more easily than the higher's. The lower LUMO energy in other words lower LUMO–HOMO energy gap (ΔE) affects the noncovalent binding affinities of the compounds to biological molecules as receptor [61].

3.4. Electrochemical measurements

The voltammetric measurements of the Cu(II) complex were carried out on glassy carbon electrode in DMF, tetrabutylammonium tetrafluoroborate as supporting electrolyte by cyclic voltammetry. The electrochemical behavior of Cu(II) complex showed both the oxidation and reductions half waves labeled O and R, with in the electrochemical window of DMF containing 0.1 M TBAFB. All These processes can be attributed to successive addition and removal of one electron to the molecule. Cyclic voltammograms of the complex showed that, both oxidation and reduction half wave potentials that are (O) oxidation at −0.45 V and (R) reduction at −1.15 V are found to be irreversible. Ligand is electrochemically in active in the electrochemical window of the solvent (Fig. 3).

3.5. Biological studies

3.5.1. Antibacterial activity results

The test compounds were screened in vitro for their antibacterial activities against four Gram-positive species (*S. aureus*, *B. subtilis B. cereus* and *E. faecalis*) and three Gram-negative species (*E. Coli*, *P. Aeruginosa* and *K. pneumonia*) by the disc diffusion and micro dilution methods. The antibacterial results were given in Table 6 by disc diffusion and Table 7 by micro dilution methods. The results were compared with those of the standard drugs as sulfamethoxazole and sulfisoxazole (Figs. 4 and 5). The size of the inhibition zone depends upon the culture medium, incubation conditions, rate of diffusion and the concentration of the antibacterial agent (the activity increases as the concentration increases). In the present study, the Absh and its Cu(II) complex are active against both types of the bacteria, which may indicate broad-spectrum properties. The remarkable activity of these compounds may be arising from the sulfonamide group, which may play an important role in the antibacterial activity.

As the disc diffusion assay results evidently show that Cu(II) complex exhibits strong inhibition effect against tested bacteria whereas the ligand Absh has moderate activity (Table 6, Figs. 4 and 5). Absh and its Cu(II) complex show the highest activities against Gram-positive *bacteria E. faecalis* in the diameter zone of 11 and 13 mm whereas sulfisoxazole and sulfamethoxazole, the drug used as standard, have been found inactive.

The Cu(II) complex shows remarkable increase in antibacterial activity than the parent ligand, Absh. Percentage of inhibition for the compounds exhibited in Fig. 5 that is expressed as excellent activity (120–200% inhibition), good activity (90–100% inhibition), moderate activity (75–85% inhibition), significant activity (50–60% inhibition), negligible activity (20–30% inhibition) and no activity [62]. As seen in Fig. 5, the ligand Absh (175%) and its Cu(II) complex (187%) show excellent activity against Gram-negative bacteria *P. aeruginosa.* And also, the compounds exhibit moderate or significant activity against the other tested *bacteria* (Sulfisoxazole is accepted 100% inhibition).

According to the MIC's results shown in Table 7, the compounds possess a broad spectrum of activity against the tested bacteria at the concentrations of 62.50–500 μg/mL [63]. The Cu(II) complex shows good activity against all of Gram-positive *bacteria (B. subtilis ATCC*, *B. cereus NRRL-B*, *E. Faecalis and ATCC S. aureus ATCC) and* Gram-negative bacteria (only *P. aeruginosa ATCC)* whereas sulfisoxazole has less activity or no activity against test bacteria.

Cu(II) complex has significant activity on the growth of bacteria as shown in Tables 6 and 7. It is proposed that the increasing in lipophilic character of metal complex may be responsible for its potent antibacterial activity than ligand. The permeation of Cu(II) complex through the lipid layer of the cell membranes deactivates diverse cellular enzymes, which play a vital role in various biologic systems of these bacteria [64–66].

3.5.2. CA(II) enzyme inhibition result

In this study, our aim was to determine the inhibitory effects of new the ligand, Absh and its Cu(II) complex. The inhibitory effects of new compounds were evaluated by using IC_{50} (IC_{50} represents the molarity of inhibiting a 50% decrease of enzyme activity) and K_i (inhibitor–enzyme dissociation constant) values which are two of the most appropriate parameters of the inhibitors (Table 8) [67]. Acetazolamide (5-acetamido-1,3,4-thiadiazole-2-sulfonamide) (AAZ) has also been investigated as standard inhibitor, clinically used against CAII. As seen in Table 8 and Figs. 6a and 6b, the compounds behave as inhibitors against hCA II enzyme. In addi-

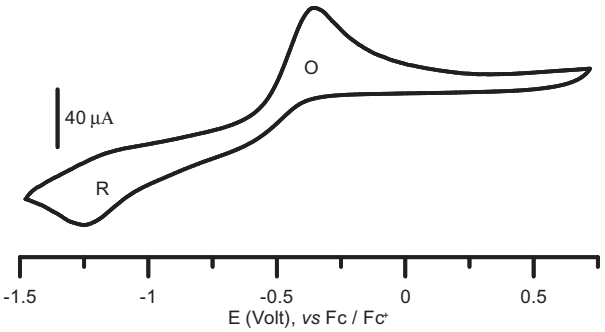

Fig. 3. Cyclic voltammogram of Cu(II) complex in DMF containing 0.1 M TBAFB, scan rate: 100 mV/s.

Table 5
Calculated ionisation potential (I), electron affinity (A), energy band gap (ΔE), electronegativity (χ), chemical potential (μ), global hardness (η), global softness (S) and global electrophilicity index (ω) for Absh and Cu(II) complex in eV.

Compound	I	A	ΔE	χ	μ	η	S	ω
L	7.527	0.6065	6.9205	4.0668	−4.0668	3.4602	0.2890	2.3899
$Cu[L_2(CH_3COO)_2]$	7.0312	2.0762	4.9550	4.5537	−4.5537	2.4775	0.8072	3.7329

Table 6
Inhibition zone values (mm) of Absh and its Cu(II) complex by disc diffusion method.

Compound	*B. subtilis* ATCC	*B. cereus* NRRL-B-	*E. faecalis* ATCC	*S. aureus* ATCC	*P. aeruginosa* ATCC	*K. pneuonia* ATCC	*E. coli* ATCC
L	9	12	11	11	14	12	12
$Cu[L_2(CH_3COO)_2]$	12	14	13	13	15	14	13
Sulfisoxazole	25	18	–	17	8	20	28
Sulfamethoxazole	15	15	–	18	17	17	24

Reference: Sulfisoxazole, Sulfamethoxazole.

Table 7
The MIC's (μg/mL)values of Absh and its Cu(II) complex by micro dilution method.

Compound	*B. subtilis* ATCC	*B. Cereus* NRRL-B-	*E. faecalis* ATCC	*S. aureus* ATCC	*P. aeruginosa* ATCC	*K. pneuonia* ATCC	*E. coli* ATCC
L	500	125	125	125	62.5	125	125
$Cu[L_2(CH_3COO)_2]$	125	125	62.5	62.5	62.5	62.5	125
Sulfisoxazole	–	375	93.75	93.75	375	23.4	23.4
Sulfamethoxazole	1500	16	32	32	64	16	64

Reference: sulfisoxazole, sulfamethoxazole.

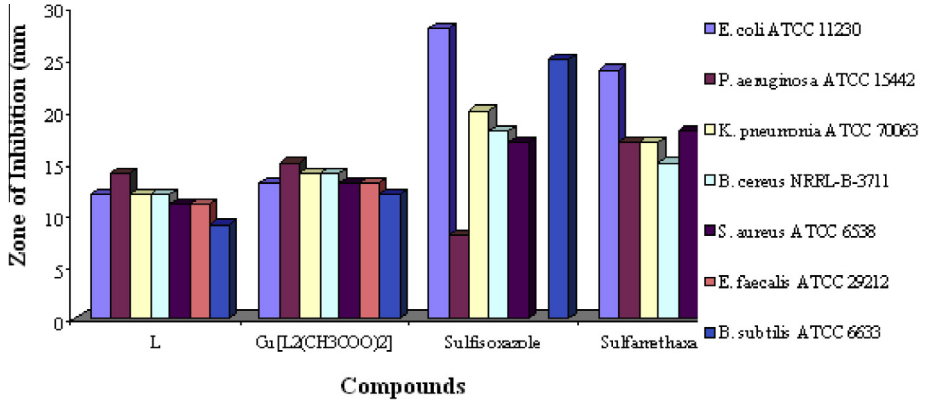

Fig. 4. Comparison of antibacterial activity of ligand, Cu(II) complex and antibiotics.

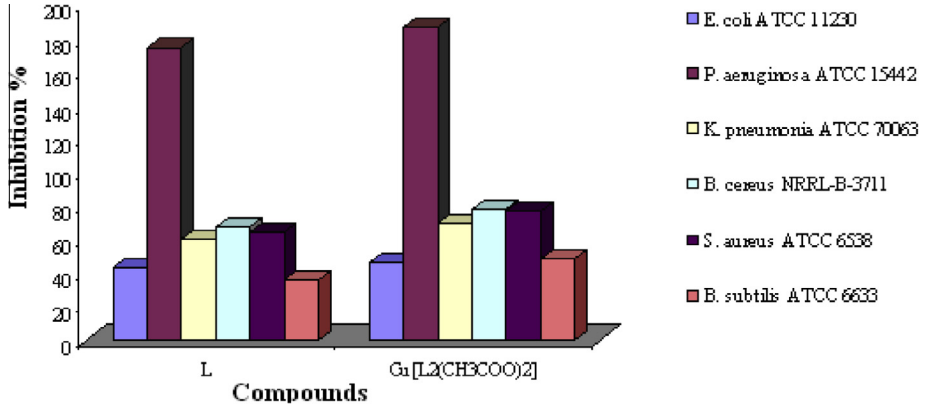

Fig. 5. Percentage of inhibition of ligand and metal (II) complex against sulfisoxazol.

tion, Cu(II) complex shows remarkable inhibition effect (K_i: 7,23 × 10^{-6} M, IC_{50}:1.85 × 10^{-4}) on hCA II than the ligand which is probably due to the further effect of the Cu(II) ion on the histidine residue in the active site of CAII enzyme [68,69].

3.5.3. In vitro antitumor activity

The compounds, Absh and its Cu(II) complex were evaluated against breast cancer cell lines MCF-7 (estrogen responsive proliferative breast cancer model) cells using MTT assay to assess cell proliferation. The results find out that Cu(II) complex shows efficient antiproliferative activity by inhibiting cell growth with IC_{50} values in the micromolar range, are shown in Table 9. Among the active compounds, the Cu(II) is found to inhibit growth of MCF-7 cells at IC_{50} significantly near to the standard anticancer agent docetaxel. On the other hand, the higher potency of Cu(II) complex than ligand may be due to many reasons, the coordination of Absh with Cu(II)

Table 8
The result of inhibition studies for Absh and its Cu(II) complex on carbonic anhydrase II.

Compound	hCA II Esterase activity	
	IC_{50} (M)	K_i (M)
L	2.73×10^{-4}	2.10×10^{-4}
$Cu[L_2(CH_3COO)_2]$	1.85×10^{-4}	1.48×10^{-4}
Acetazolamide	1.13×10^{-4}	1.07×10^{-4}

Reference: acetazolamide.

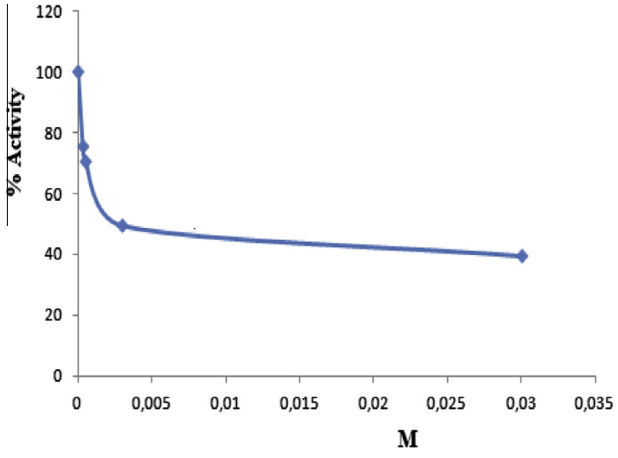

Fig. 6a. Activity% [Absh] regression analysis graphs for hCA II in presence 5 different Absh concentrations.

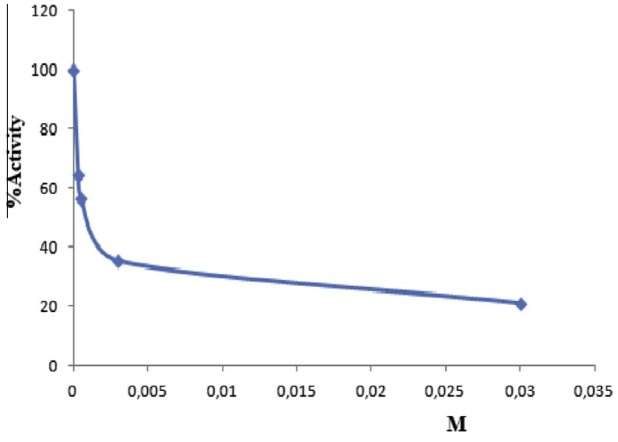

Fig. 6b. Activity % [Cu(II) complex] regression analysis graphs for hCA II in presence 5 different Cu(II) complex concentrations.

Table 9
Cell growth inhibitory effect of Absh and its Cu(II) complex and their IC_{50} values (l M in MCF-7 cell lines).

Compound	IC_{50} (μmol L^{-1})
L	10.27
$Cu[L_2(CH_3COO)_2]$	8.01
Docetaxel	7.24

Reference: docetaxel.

ion. As it is known that Cu(II) is an essential element in human normal metabolism because its functions as cofactor of several metalloenzymes [70,71] or its suitable molecular size and its distorted octahedral geometry.

4. Conclusions

In this study, we have reported the synthesis of sulfonamide derivative and its Cu(II) complex. The structural characterizations of the synthesized compounds were made by using the elemental analyses, spectroscopic methods, electrochemical, magnetic and conductance studies. The structure of N′-Acetyl butane sulfonic acid hydrazide (Absh) was also supported by X-ray crystal diffraction studies. From the spectroscopic characterization, it is concluded that the ligand, Absh acts as a bidentate ligand, coordinating through >C═O and NH bonded to SO_2. Based on physicochemical evidence, the proposed structure of Cu(II) complex is exhibited in Fig. 2. The biological activity screening shows that Cu(II) complex has high inhibition effect against tested bacteria, CA II enzyme and breast cancer cell lines MCF-7. The calculated electronic descriptors correlate the good activity trend of Cu(II) complex.

Acknowledgements

This research was supported by Gazi University Research Found under Project No. 05/2010-92 and TUBITAK Project No. 105T240. We thank Ankara University, Faculty of Pharmacy. Central Labs for allocation of time at the Mass Spectra and Elemental Analyses.

Appendix A. Supplementary material

CCDC 1003393 contain the supplementary crystallographic data for this paper. These data can be obtained free of charge from The Cambridge Crystallographic Data Centre via www.ccdc.cam.ac.uk/data_request/cif. Supplementary data associated with this article can be found, in the online version, at http://dx.doi.org/10.1016/j.ica.2014.09.033.

References

[1] J. Borras, G. Alzuet, S. Ferrer, C.T. Supuran, in: C.T. Supuran, A. Scozzafava, J. Conway (Eds.), Carbonic Anhydrase: Its Inhibitors and Activators, vol. 36, CRC Press, Boca Raton, FL, 2004, pp. 183–207.
[2] A.K. Gadad, C.S. Mahajanshetti, S. Nimbalkar, A. Raichurkar, Eur. J. Med. Chem. 35 (2000) 853.
[3] L. Saiz-Urra, M.P. Gonzalez, I.G. Collado, R. Hernandez-Galan, J. Mol. Graph. Model. 25 (2007) 680.
[4] V.K. Agrawal, R. Srivastava, P.V. Khadikar, Bioorg. Med. Chem. 9 (2001) 3287.
[5] M. Jaiswal, P.V. Khadikar, A. Scozzafava, C.T. Supuran, Bioorg. Med. Chem. Lett. 14 (2004) 3283.
[6] S. Samanta, K. Srikanth, S. Banerjee, B. Debnath, S. Gayen, T. Jha, Bioorg. Med. Chem. 12 (2004) 1413.
[7] C.T. Supuran, A. Scozzafava, Expert Opin. Ther. Pat. 10 (2000) 575.
[8] T.H. Maren, Annu. Rev. Pharmacol. 16 (1976) 309.
[9] C.W. Thornber, Chem. Soc. Rev. 8 (1979) 563.
[10] W. de Keizer, M.E. Bienenmann-Ploum, A.A. Bergwerff, W. Haasnoot, Anal. Chim. Acta 620 (2008) 142.
[11] A. Innocenti, A. Maresca, A. Scozzafava, C.T. Supuran, Bioorg. Med. Chem. Lett. 18 (2008) 3938.
[12] K.K. Sahu, V. Ravichandran, V.K. Mourya, R.K. Agrawal, Med. Chem. Res. 15 (2007) 418.
[13] H.A. Seow, P.G. Penketh, K. Shyam, S. Rockwell, A.C. Sartorelli, Proc. Natl. Acad. Sci. 102 (2005) 9282.
[14] A. Kamal, M.N.A. Khan, K.S. Reddy, K. Rohini, Bioorg. Med. Chem. 15 (2007) 1004.
[15] A.M. Al-Azzawi, M.S.A. Razzak, Kerbala J. Pharm. Sci. 2 (2011) 124.
[16] S.M. Sondhi, M. Dinodia, S. Jain, A. Kumar, Indian J. Chem. 48 (2010) 1128.
[17] A. Ignat, V. Zaharia, C. Mogoşan, N. Palibroda, C. Cristea, L. Silaghi-Dumitrescu, Farmacia 58 (2010) 290.
[18] M.R. Abdo, D. Vullo, M.C. Saada, J.L. Montero, A. Scozzafava, J.Y. Winum, et al., Bioorg. Med. Chem. Lett. 19 (2009) 2440.
[19] J.E.F. Reynolds (Ed.), Martindale: The Extra Pharmacopoeia, Royal Pharmaceutical Society, London, 1996.
[20] G. Casanova, G. Alzuet, J. Borras, S. Garcıa-Granda, I. Candano Gonzalez, J. Inorg. Biochem. 56 (1994) 65.
[21] Z.H. Chohan, K. Mahmood-Ul-Hassan, M. Khan, C.T. Supuran, J. Enzyme Inhib. Med. Chem. 20 (2005) 183.

[22] G.V. Tsintsadze, R.S. Kurtanidze, M.A. Mdivani, A.P. Narimanidze, in: L.N. Mazalov (Ed.), Problemy Sovremennoy Bioneorganicheskoy, Khimii, Nauka, Novasibirskiy, (1986) 211.
[23] N.I. Dodoff, U. Ozdemir, N. Karacan, M. Georgieva, S.M. Konstantinov, M.E. Stefanova, Z. Naturforsch. 54 (1999) 1553.
[24] O.S. Şentürk, U.O. Ozdemir, S. Sert, N. Karacan, F. Uğur, Inorg. Chem. Commun. 6 (2003) 926.
[25] S. Sert, O.S. Şentürk, U.O. Ozdemir, N. Karacan, F. Uğur, J. Coord. Chem. 57 (2003) 183.
[26] U.O. Ozdemir, N. Akkaya, N. Özbek, Inorg. Chim. Acta 400 (2013) 13.
[27] U. Ozdemir, P. Güvenç, E. Şahin, F. Hamurcu, Inorg. Chim. Acta 362 (2009) 2613.
[28] U. Ozdemir, F. Arslan, F. Hamurcu, Spectrochim. Acta, Part A 75 (2010) 121.
[29] U.O. Ozdemir, G. Olgun, Spectrochim. Acta, Part A 70 (2008) 641.
[30] U. Ozmen Ozdemir, A. Altuntaş, A. Balaban, F. Arslan, F. Hamurcu Gündüzalp, Spectrochim. Acta, Part A 128 (2014) 452.
[31] G.M. Sheldrick, SHELXS97 and SHEXL97. Program for Crystal Structure Solution and Refinement. University of Göttingen, Germany, (1997).
[32] Stoe & Cie, X-AREA (Version 1.18) and X-RED32 (Version 1.04). Stoe & Cie, Darmstadt, Germany, (2002).
[33] L.J. Farrugia, J. Appl. Cryst. 30 (1997) 565.
[34] A.D. Becke, J. Phys. Chem. 9 (8) (1993) 5648.
[35] C. Lee, W. Yang, R.G. Parr, Phys. Rev. B 37 (1998) 785.
[36] A.W. Ehlers, M. Bohme, S. Dapprich, A. Gobbi, A. Hollwarth, V. Jonas, K.F. Kohler, R. Stegmann, A. Veldkamp, G. Frenking, Chem. Phys. Lett. 208 (1993) 111.
[37] J. Tomasi, B. Mennucci, E. Cance, Theochem 464 (1999) 211.
[38] M.J. Frisch, G.W. Trucks, H.B. Schlegel, G.E. Scuseria, M.A. Robb, J.R. Cheeseman, G. Scalmani, V. Barone, B. Mennucci, G.A. Petersson, H. Nakatsuji, M. Caricato, X. Li, H.P. Hratchian, A.F. Izmaylov, J. Bloino, G. Zheng, J.L. Sonnenberg, M. Hada, M. Ehara, K. Toyota, R. Fukuda, J. Hasegawa, M. Ishida, T. Nakajima, Y. Honda, O. Kitao, H. Nakai, T. Vreven, J.A. Montgomery Jr., J.E. Peralta, F. Ogliaro, M. Bearpark, J.J. Heyd, E. Brothers, K.N. Kudin, V.N. Staroverov, R. Kobayashi, J. Nor-mand, K. Raghavachari, A. Rendell, J.C. Burant, S.S. Iyengar, J. Tomasi, M. Cossi, N. Rega, J.M. Millam, M. Klene, J.E. Knox, J.B. Cross, V. Bakken, C. Adamo, J. Jaramillo, R. Gomperts, R.E. Stratmann, O. Yazyev, A.J. Austin, R. Cammi, C. Pomelli, J.W. Ochterski, R.L. Martin, K. Morokuma, V.G. Zakrzewski, G.A. Voth, P. Salvador, J.J. Dannenberg, S. Da rich, A.D. Daniels, O. Farkas, J.B. Foresman, J.V. Ortiz, J. Cioslowski, D.J. Fox, Gaussian 09, Revision A.02, Gaussian Inc, Wallingford, CT (2009).
[39] R. Dichfield, Mol. Phys. 27 (1974) 789.
[40] R.B. Mulaudzi, A.R. Ndhlala, M.G. Kulkarni, J.F. Finnie, J. Van Staden, J. Ethnopharmacol. 135 (2011) 330.
[41] S.G. Küçükgüzel, A. Mazi, F. Sahin, S. Öztürk, J. Stables, Eur. J. Med. Chem. 38 (2003) 1005.
[42] J. McD Armstrong, Direcck V. Myers, Jacob A. Verpoorte, John T. Edsall, J. Biol. Chem. 241 (1966) 5137.
[43] S.L. Bradbury, J. Biol. Chem. 244 (1969) 2002.
[44] C. Temperini, A. Scozzafava, L. Puccetti, C.T. Supuran, Bioorg. Med. Chem. Lett. 15 (2005) 5136.
[45] F. Denizot, R. Lang, J. Immunol. Methods 89 (1986) 271.
[46] W.L.F. Armarego, C.L.L. Chai, Purification of Laboratory Chemicals, fifth ed., Butterworth/Heinemann, Tokyo, 2003.
[47] E. Tas, A. Kilic, N. Konak, I. Yilmaz, Polyhedron 27 (2008) 1024.
[48] S. AbouEl-Enein, F.A. El-Saied, S.M. Emam, M.A. Ell-Salamony, Spectrochim. Acta, Part A 71 (2008) 421.
[49] S. Alyar, U.O. Ozmen, N. Karacan, O.S. Şentürk, K.A. Udachin, J. Mol. Struct. 889 (2008) 144.
[50] A. Balaban, N. Çolak, H. Ünver, B. Erk, T.N. Durlu, D.M. Zengin, J. Chem. Cryst. 38 (2008) 369.
[51] A. Balaban, B. Erk, Rus. J. Inorg. Chem. 55 (2010) 1094.
[52] A. Balaban, N. Özbek, N. Karacan, Med. Chem. Res. 21 (2012) 3435.
[53] K. Nakamoto, Infrared and Raman Spectra of Inorganic and Coordination Compounds, 4th ed., Wiley, New York, 1986.
[54] Z. Karagoz, M. Genc, E. Yılmaz, S. Keser, Spect. Let. 46 (2013) 182.
[55] K.D. Pulak, P. Sadhan, L. Tian-Huay, G.B.D. Mike, C. Pabitra, Polyhedron 23 (16) (2004) 2457.
[56] A. Golcu, M. Tumer, H. Demirelli, R.A. Wheatley, Inorg. Chim. Acta 358 (2005) 1785.
[57] S. Alyar, N. Ozbek, N. Ocak, Med. Chem. Res. 22 (2013) 2051.
[58] R.L. Dutta, A. Syamal, Elements of Magnatochemistry, second ed., East West Press, New Delhi, 1996.
[59] R.N. Patel, N. Singh, K.K. Shukla, U.K. Chauhan, S. Chakraborty, J.N. Gutierrez, A. Castineiras, J. Inorg. Biochem. 98 (2004) 231.
[60] R.C. Santana, J.F. Carvalho, I. Vencato, H.B. Napolitano, A.J. Bortoluzzi, G.E. Barberis, R.E. Rapp, M.C.G. Passeggi, R. Calvo, Polyhedron 26 (2007) 5001.
[61] A.B. Gündüzalp, U.O. Ozmen, B.S. Çevrimli, S. Mamaş, S. Çete, Med. Chem. Res. 23 (2014) 3255.
[62] N. Sultana, A. Naz, M.S. Arayne, M.A. Mesaik, J. Mol. Struct. 969 (2010) 17.
[63] Z.H. Chohan, A.U. Shaikh, M.M. Nasee, C.T. Supuran, J. Enzyme Inhib. Med. Chem. 21 (2006) 771.
[64] Z.H. Chohan, A. Scozzafava, C.T. Supuran, J. Enzyme Inhib. Med. Chem. 17 (2002) 261.
[65] Z.H. Chohan, C.T. Supuran, A. Scozzafava, J. Enzyme Inhib. Med. Chem. 18 (2003) 1.
[66] F. Hamurcu, A. Balaban Gündüzalp, S. Çete, B. Erk, Trans. Met. Chem. 33 (2008) 137.
[67] O. Arslan, İ.Ö. Küfrevioğlu, B. Nalbantoğlu, Bioorg. Med. Chem. 15 (1997) 515.
[68] P.V. Khadikar, S. Joshi, S.G. Kashkhedikar, B.D. Heda, Indian J. Pharm. Sci. 46 (1984) 209.
[69] S. Lindskog, Pharmacol. Ther. 74 (1997) 1.
[70] M. Gocke, S. Utku, S. Gur, A. Rozkul, F. Gumus, Eur. J. Med. Chem. 40 (2005) 135.
[71] F. Saczewski, E. Dziemidowicz-Borys, P.J. Bednarski, R. Grunert, M. Gdaniec, P. Tabin, J. Inorg. Biochem. 100 (2006) 1389.